

Unprecedented High Temperature CO₂ Selectivity and Effective Chemical Fixation by a Copper-Based Undulated Metal–Organic Framework

Prasenjit Das and Sanjay K. Mandal*



Cite This: *ACS Appl. Mater. Interfaces* 2020, 12, 37137–37146



Read Online

ACCESS |

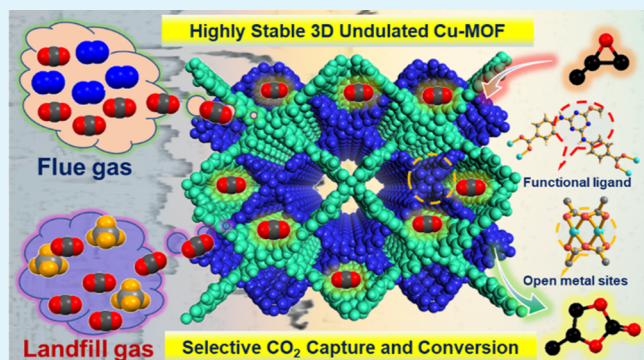
Metrics & More

Article Recommendations

Supporting Information

ABSTRACT: Post- and precombustion CO₂ capture and separation are the vital challenges from industrial viewpoint, as the accessible technologies are not cost-effective and cumbersome. Thus, the development of functional metal–organic frameworks (MOFs) that are found to be promising materials for selective CO₂ capture, separation, and conversion is gaining an importance in the scientific world. Based on the strategic design, a new functionalized triazine-based undulated paddle-wheel Cu-MOF (**1**), $\{[\text{Cu}(\text{MTABA})(\text{H}_2\text{O})]\cdot 4\text{H}_2\text{O}\cdot 2\text{EtOH}\cdot \text{DMF}\}_n$ (where, H₂MTABA = 4,4'-(6-methoxy-1,3,5-triazine-2,4-diyl)bis(azanediyl)dibenzoic acid), has been synthesized under solvothermal conditions and fully characterized. MOF **1** contains a one-dimensional channel along the *a*-axis with pore walls decorated with open metal sites, and multifunctional groups (amine, triazine, and methoxy). Unlike other porous materials, activated **1** (**1'**) possesses exceptional increment in CO₂/N₂ and CO₂/CH₄ selectivity with increased temperature calculated by the ideal adsorbed solution theory. With an increase in temperature from 298 to 313 K, the selectivity of CO₂ rises from 350.3 to 909.5 at zero coverage, which is unprecedented till date. Moreover, **1'** behaves as a bifunctional heterogeneous catalyst through Lewis acid (open metal) and Brønsted acid sites to facilitate the chemical fixation of CO₂ to cyclic carbonates under ambient conditions. The high selectivity for CO₂ by **1'** even at higher temperature was further corroborated with configurational bias Monte Carlo molecular simulation that ascertains the multiple CO₂-philic sites and epoxide binding sites in **1'** to further decipher the mechanistic pathway.

KEYWORDS: undulated metal–organic framework, paddle-wheel structure, high temperature CO₂ selectivity, CBMC simulation, CO₂ conversion, bifunctional heterogeneous catalysis



INTRODUCTION

The climate destabilization has become a vital and challenging environmental issue owing to greenhouse gas emissions. More markedly, carbon dioxide (CO₂) discharge into the environment is enormously increasing and creating a scarcity problem, according to a NASA's report (2017).^{1,2} In addition to an innate process such as respiration and natural processes such as volcanic eruptions, anthropogenic activities mainly industrialization, deforestation, fossil-fuel power plants, and automobile toxic emissions are the culprit for global warming.³ Therefore, emitted CO₂ into the atmosphere will have a remarkable impact on the global CO₂ concentration. Thus, the development of technologies related to CO₂ capture and sequestration is imperial for efficient CO₂ capture. Under this canvas, CO₂-philic porous materials are highly demanding for selective CO₂ sorption and storage from pre-and postcombustion processes.⁴ In this regard, preferential adsorption of CO₂ over N₂ at elevated temperatures (313–333 K) with amplified selectivity is a requisite during postcombustion of flue gas.^{5–9} In addition to it, the proper implementation of captured CO₂ as a

recyclable carbon feedstock for chemical transformation into value-added products is equally essential to mitigate the global warming problem. Primarily, the cycloaddition of CO₂ with epoxides to produce cyclic carbonates without any byproduct formation has been regarded as one of the intriguing green and atom economy processes.^{10–12} These cyclic carbonates serve as key industrial intermediates in pharmaceuticals, electrolytes, and petrochemicals.^{13,14} Moreover, the kinetic inertness and thermodynamic stability of CO₂ poses a synthetic challenge during the transformation process. Concurrently, it is desired to dedicate considerable efforts for developing CO₂-philic porous materials that can serve as potential heterogeneous

Received: May 17, 2020

Accepted: July 20, 2020

Published: July 20, 2020



catalysts for the chemical conversion of CO₂ under ambient conditions.^{15–19}

Recently, metal–organic frameworks (MOFs) have become emanating candidates of highly crystalline porous materials constructed from inorganic metal nodes and organic building units.²⁰ Owing to their large surface area, tailor-made pores, tunable functionality, and high chemical and thermal stability, these materials are very attractive toward CO₂ sorption, separation, and conversion processes.^{21–32} The robust nature and chemo-stability of these frameworks with efficient CO₂ capture plays a crucial role in heterogeneous catalytic activity with facile product isolation and good recyclability. Additionally, several strategies that have been adopted in the design of MOFs to enhance the CO₂ uptake and chemical conversion performance include the following: (i) the presence of open metal sites (OMSs) or creation of OMSs by the removal of coordinated solvent molecules, as Lewis acid centers, and (ii) the incorporation of functional moieties such as nitrogen-rich centers as Lewis basic or Brønsted acidic sites and polar groups.^{33–41} Also, the availability of pores permits the entry of epoxide substrates to undergo reaction with adsorbed CO₂.⁴² Till date, different MOFs have shown good catalytic activity for the CO₂ conversion to cyclic carbonates at elevated temperatures (>80 °C) and pressures (>2 MPa).^{43–45} Only a few MOFs were reported to show high catalytic efficiency under ambient conditions.⁴⁶ Thus, the design of MOFs for highly efficient CO₂ fixation under ambient conditions is still a challenging and vital task.

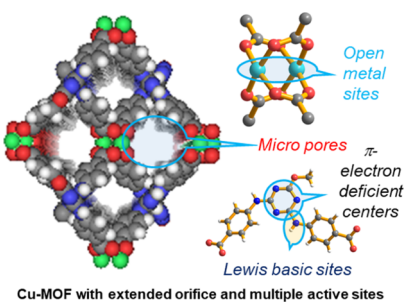
To achieve the above-mentioned targets, we have prepared a triazine-based, and methoxy- and amine-functionalized dicarboxylic acid, 4,4'-(6-methoxy-1,3,5-triazine-2,4-diyl)bisc(azanediyl)dibenzoic acid (H₂MTABA). Using H₂MTABA, a porous thermally and chemically stable multifunctional three-dimensional undulated MOF, {[Cu(MTABA)(H₂O)]·4H₂O·2EtOH·DMF}_n (**1**), has been prepared under solvothermal conditions to showcase its unprecedented selectivity of CO₂ over N₂ and CH₄ at higher temperature (Scheme 1), which has

RESULTS AND DISCUSSION

Synthesis and Structural Characterization. H₂MTABA ligand was synthesized in two steps from cyanuric chloride and characterized by high-resolution mass spectrometry, nuclear magnetic resonance (NMR), and Fourier transform infrared (FTIR) spectroscopy (Scheme S1, Figures S1–S3). Compound **1** was synthesized from a mixture of Cu(NO₃)₂·4H₂O and H₂MTABA in a DMF/EtOH/H₂O (1:1:1) mixture at 120 °C for 48 h followed by slowly cooling to room temperature in 36 h. Block-shaped blue crystals were obtained in 85% yield (Scheme S2). In its FTIR spectrum (Figure S4), the asymmetric and symmetric carboxylate stretching frequencies were identified at 1590 and 1424 cm⁻¹, respectively, to evaluate the carboxylate binding modes to the Cu(II) centers. A difference value of 166 cm⁻¹ between the asymmetric and symmetric stretches indicated the presence of a paddle-wheel core in **1**,⁴⁷ as confirmed by the single crystal X-ray diffraction.

Compound **1** crystallizes in the monoclinic C2/m space group (no. 12) (Table S1). One Cu(II) center, one MTABA, and one coordinated H₂O molecule are present in the asymmetric unit. The pentacoordinated Cu(II) center in **1** displays a slightly distorted square pyramidal geometry ($\tau = 0.035$) with a typical {Cu₂(OCO)₄} paddle-wheel core (Figure 1a), the secondary building unit (SBU). The paddle-wheel SBU is constructed from eight oxygen atoms of four different carboxylate groups of MTABA and one oxygen atom of the coordinated water. The Cu(II)...Cu(II) distances observed in **1** are 2.644 Å (within the paddle-wheel core) and 16.381 Å (between the paddle-wheel units). The Cu–O_{carb} and Cu–O_{water} distances are found to be 1.970 and 2.073 Å, respectively. Each paddle-wheel SBU is connected to four other such units via the full span of four MTABA ligands resulting in a two-dimensional (2D) net. The undulated nature of two such square-shaped 2D nets generates a three-dimensional (3D) parallel polycatenated undulated framework (Figure 1b).⁴⁸ For the topological analysis, the structure of **1** is simplified, where the paddle-wheel SBU acts as a tetraconnected node and the ligand MTABA acts as a disconnected bent linker (Figure 2). Using the TOPOS17 program, a node and linker representation shows that the framework has a 4-connected uninodal, sq1/Shubnikov tetragonal plane net topology with the Schläfli point symbol {4⁴.6²} (Figure 2). Two different 1D channels were formed along *a*-axis with pore dimensions (excluding van der Waals radii) of 12.305 × 9.612 and 9.68 × 9.54 Å². These channels are filled with disordered solvent molecules (four water, two ethanol, and one DMF) that were squeezed out for the refinement of the structure. This is supported by the elemental analysis and thermogravimetric analysis (TGA) data. All pore walls are adorned with amine, triazine, and methoxy groups of the ligand as well as OMSs from different undulated layers.

Thermal, Physical, and Surface Properties. The thermal stability of **1** was introspected by TGA to reveal its high stability up to 350 °C after the loss of solvent molecules [four lattice water, one coordinated water and two ethanol (calcd 26.1%, found 26.5%) from 30 to 200 °C, and one DMF (calcd 10.04%, found 10.12%) from 200 to 390 °C] (Figure S5). This clearly corroborates with its single crystal structure. Moreover, the well-matched simulated and experimental powder X-ray diffraction (PXRD) patterns validated the bulk phase purity of **1** (Figure S6). To confirm its hydrolytic stability of **1**, the PXRD patterns obtained after soaking in



Scheme 1. Multifunctional Microporous Cu-MOF: OMSs, Amine-, and Methoxy-Functionalized Ligand with a π-Electron-Deficient Triazine Center

been followed by the ideal adsorbed solution theory (IAST). The high CO₂ capture and its efficient conversion to cyclic carbonates is attributed to the presence of Lewis acid OMSs and Brønsted acid sites to facilitate chemical fixation of CO₂ to cyclic carbonates at room temperature and atmospheric pressure. Configurational bias Monte Carlo (CBMC) molecular simulation has further provided excellent correlation for the selective CO₂ uptake over other gases at high temperature.

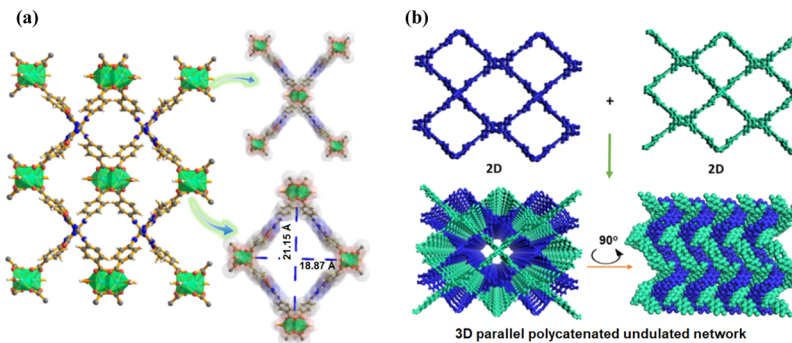


Figure 1. (a) Coordination environment and orientation of copper centers with paddle-wheel units in **1**. (b) Formation of a 3D parallel polycatenated undulated framework from two 2D square-shaped nets in **1**.

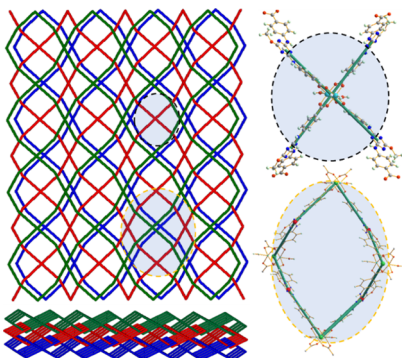


Figure 2. Topological representation of **1**.

water (for 15 days) and other protic and aprotic solvents (1 day) were also matched well with the as-synthesized pattern of **1** (Figure S7). The solid-state diffuse reflectance spectrum of **1** exhibits two bands at 279 and 322 nm corresponding to $\pi-\pi^*$ and $n-\pi^*$ transitions, respectively, and another band at 747 nm corresponding to the d-d transition (Figure S8).⁴⁹

To comprehend the surface morphology of **1**, field emission scanning electron microscopy (FESEM) was utilized. The FESEM image of **1** reflects the formation of 3D microflowers by self-assembly of 2D nanosheets, which is well-corroborated with the obtained structure (Figure 3a). The composition of **1** was further depicted by energy-dispersive X-ray (EDX) analysis and quanta area mapping study, which further illustrated the uniform distribution of Cu, C, O, and N over the entire sample (Figure 3b).

Gas Sorption Studies. The presence of inherent 1D channels and cognizable high solvent accessible void of 6955.5 Å³ (55.2% per unit cell based on PLATON) in **1** motivated us to investigate its porosity through the N₂ sorption isotherm measurement. In order to confirm complete desolvation of **1**, the FTIR and TGA of activated **1** (**1'**) were recorded and analyzed (Figure S9). As observed, no peaks due to DMF/ethanol/water are found in the FTIR and no weight loss is observed due to solvents in TGA. A sample of degassed **1'** exhibits an irreversible type I N₂ sorption isotherm according to IUPAC classification (Figure 4a). This sorption isotherm shows the microporous nature of **1** with a pore diameter of 0.9–1.2 nm (highest peak at 1.13 nm, determined by the density functional theory; Figure 4a, inset). The little broadness in the pore size is due to the flexible nature of ligand as well as several pores in that region (12.305 × 9.612 and 9.68 × 9.54 Å²). Similarly, an irreversible H₂ sorption

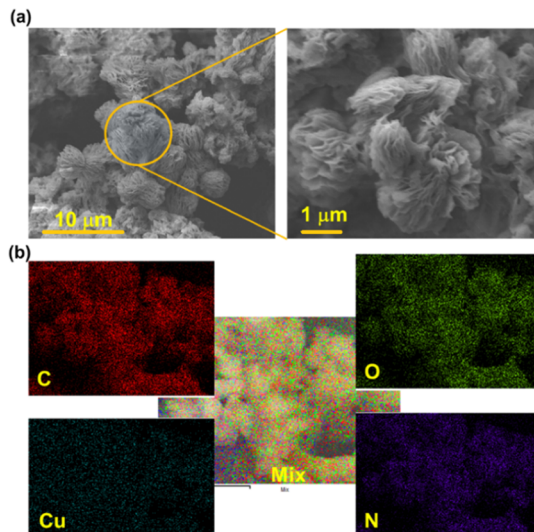


Figure 3. (a) FESEM image portraying the microflower nature of **1**. (b) EDX elemental mapping of **1**.

isotherm with a large hysteresis is observed, which corresponds to kinetic trapping (Figure S10).⁵⁰

By considering the availability of 1D channel, functional porosity, and OMSs in **1'**, it has been utilized for a clean energy application. The sorption studies of various small gases such as CO₂, N₂, and CH₄ at different temperatures have been performed. The presence of aforesaid features in the framework imbued us to assert the selective capture of CO₂ over N₂ and CH₄ (flue and landfill gases). For CO₂ sorption, type I isotherms are observed with uptakes of 24.98, 29.03, 33.62, 45.58, and 51.92 cm³ g⁻¹ (STP, at 1 bar) at 313, 305, 298, 273, and 263 K, respectively (Figure 4b). As the temperature is lowered to 195 K, **1'** exhibits a high CO₂ uptake (112.73 cm³ g⁻¹ at 1 bar), confirming its high affinity toward the framework (Figure 4c). This uptake is comparable with those for the previously reported MOFs (Table S2). The Brunauer–Emmett–Teller surface area was 349.2 m² g⁻¹ calculated from the CO₂ adsorption data at 195 K (Figure S11). Similarly, the CH₄ sorption isotherm displays uptakes of 9.36, 10.92, 11.95, 12.78, and 15.35 cm³ g⁻¹ (STP, at 1 bar) at 313, 305, 298, 273, and 263 K, respectively (Figure 4d). On the other hand, the N₂ sorption isotherm shows uptakes of 1.95, 2.77, and 3.56 cm³ g⁻¹ (STP, at 1 bar) at 313, 305, and 298 K, respectively. Moreover, for understanding the strength of interaction, the isosteric heat of adsorption (Q_{st}) of CO₂ and CH₄ at different temperatures has been estimated by

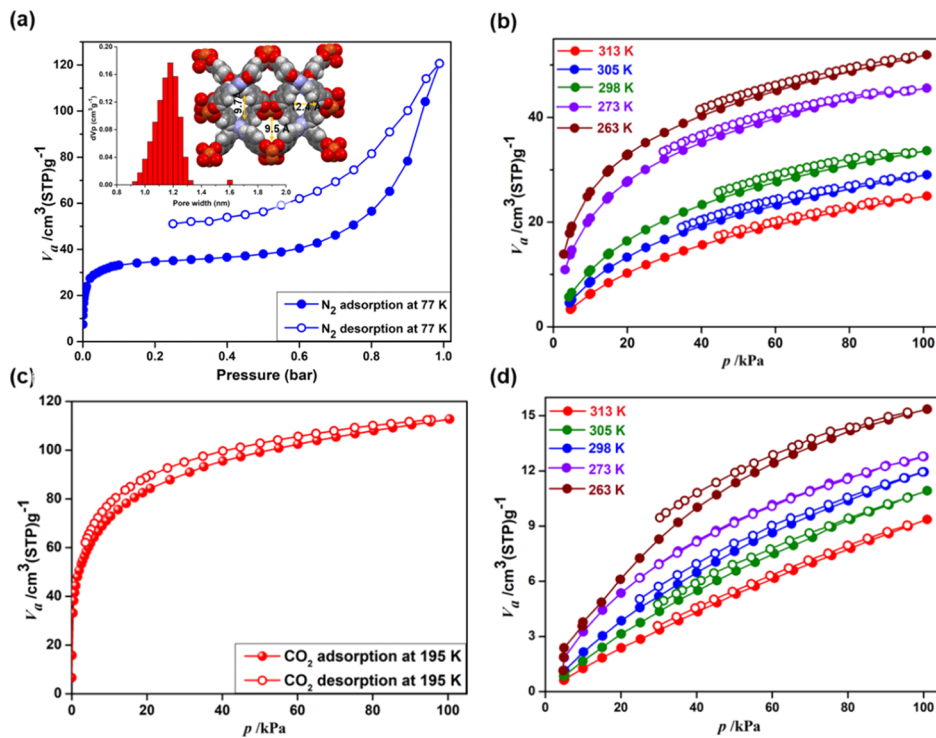


Figure 4. (a) N_2 sorption isotherm at 77 K for $1'$ (inset: pore size distribution of $1'$). (b) CO_2 sorption isotherms at 313, 305, 298, 273, and 263 K for $1'$. (c) CO_2 sorption isotherm at 195 K for $1'$. (d) CH_4 sorption isotherms at 313, 305, 298, 273, and 263 K for $1'$; (filled and open symbols indicate adsorption and desorption, respectively).

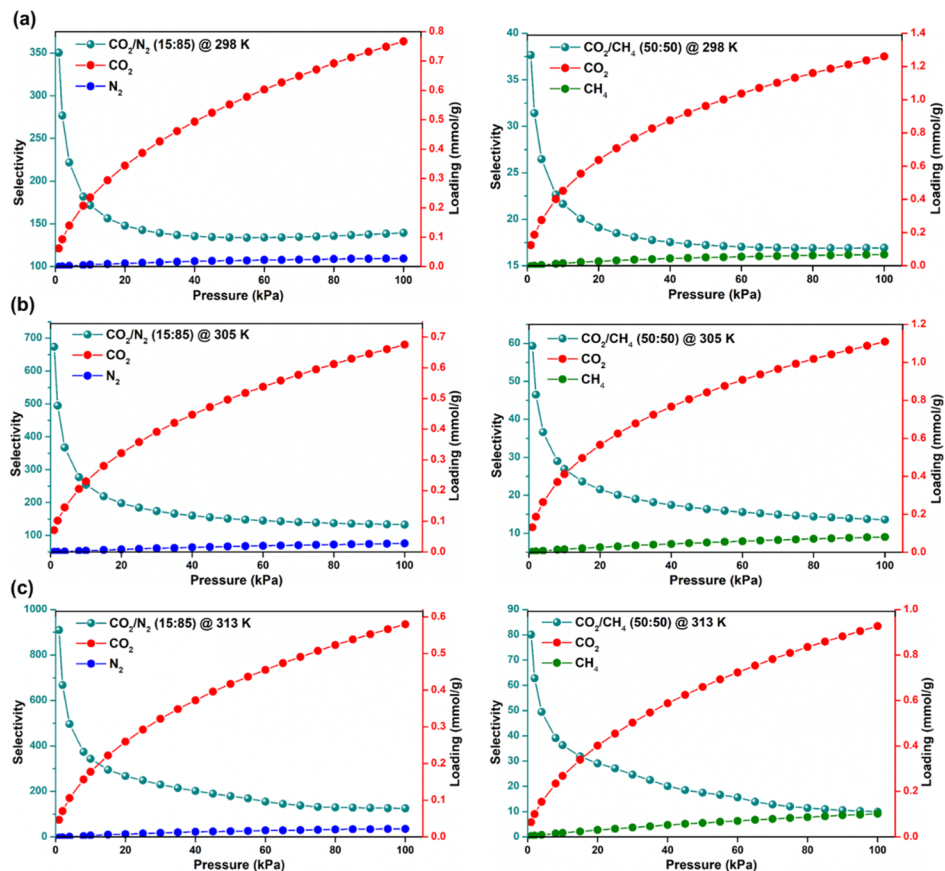


Figure 5. Loading uptake and separation selectivity enumerated by the IAST for a mixture of CO_2/N_2 (15:85) (left column) and CO_2/CH_4 (50:50) (right column) at 298 (a), 305 (b), and 313 K (c) of $1'$.

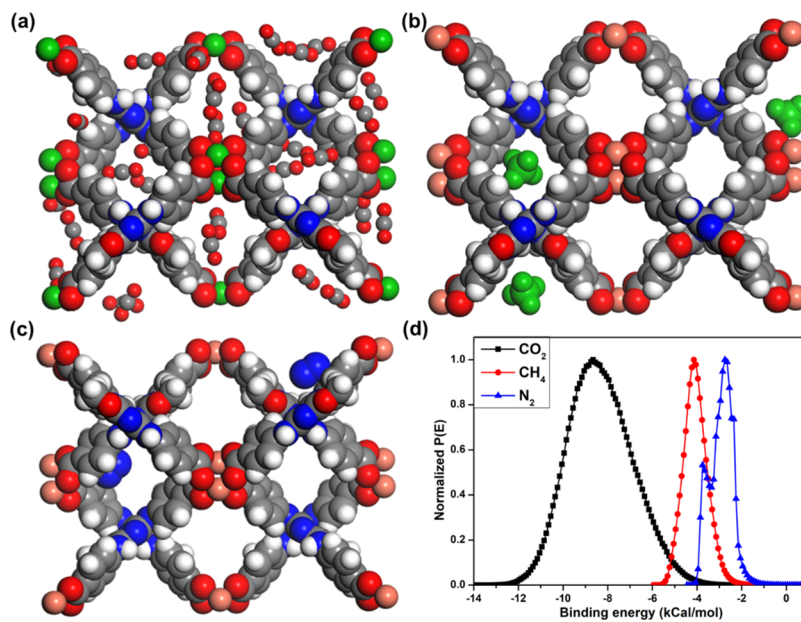


Figure 6. CBMC molecular simulation: sorption and location of (a) CO₂, (b) CH₄, and (c) N₂ on 1' at 1 bar at 313 K. (d) BE at 313 K for CO₂, CH₄, and N₂.

Clausius–Clapeyron equation and the values at zero loadings are 38.4 and 16.1 kJ mol⁻¹, respectively (Figure S12). The high Q_{st} value for CO₂ at zero coverage indicates very strong binding affinity of CO₂ with the functionalized Lewis basic and OMSs present in the micropore of 1. This Q_{st} value of CO₂ at zero coverage is comparable and higher than those reported for other MOFs (Table S3).^{51–56}

Selectivity for CO₂/N₂ and CO₂/CH₄ Mixtures by the IAST Method. The high CO₂ uptake compared to N₂ and CH₄ motivated us for further investigation of potential gas separation at different temperatures mainly at 40 °C, which is important for industrial application. To evaluate the binary separation of general feed composition of landfill gas (CO₂/N₂ = 15:85) and flue gas (CO₂/CH₄ = 50:50), IAST developed by Myers and Prausnitz has been applied.⁵⁷ First, the unary CO₂, N₂, and CH₄ isotherms at different temperatures have been fitted using the dual-site Langmuir–Freundlich (DSLF) isotherm model. Second, this DSLF fitting provides the saturation capacities (q_m), affinity coefficients (b), and deviation from an ideal homogeneous surface (n) for different gases at different temperatures. These parameters at different temperatures were taken as input into the IAST equation and the output provided the mixture adsorption equilibrium over the desired pressure range (Figures S13–S21, Table S3). The selectivity determination and loading approximation for binary gas mixtures are well-apprehended in a wide range of MOFs and zeolites using IAST in comparison with the CBMC simulations owing to their high accuracy and precision in calculation. The adsorption selectivity of CO₂/N₂ (15:85) mixture is 909.53, 673.72, and 350.35 (zero coverage) and 125.4, 132.93, and 139.55 (100 kPa) at 313, 305, and 298 K, respectively. On the other hand, the adsorption selectivity of CO₂/CH₄ (50:50) mixture is 37.65, 59.32, and 80.08 (zero coverage) and 16.92, 13.6, and 9.94 (100 kPa) at 313, 305, and 298 K, respectively (Figure 5). These six selectivity values are comparable or higher than those for other MOFs, COFs, and organic polymer-based systems, such as PCN-88 (CO₂/N₂: 18 @ 298 K, CO₂/CH₄: 5 @ 296 K), PCN-61 (CO₂/N₂: 15 @

298 K), BUT-11 (CO₂/N₂: 31.5 @ 298 K; CO₂/CH₄, 9 @ 298 K), BUT-11 (AcOH) (CO₂/N₂: 24.1 @ 298 K; CO₂/CH₄: 6.9 @ 298 K), ZIF-100 (CO₂/N₂: 25 @ 298 K and CO₂/CH₄: 5.9 @ 298 K), NOTT-202 (CO₂/N₂: 26.7 @ 273 K and CO₂/CH₄: 4.3 @ 293 K, CO₂/CH₄: 2.9 @ 273 K), TBILP-1 (CO₂/N₂: 62 @ 298 K, CO₂/CH₄: 9 @ 298 K), USTC-253-TFA (CO₂/N₂: 75 @ 298 K), SMOF-SiFSIX-1 (CO₂/N₂: 78–60 @ 298 K; CO₂/CH₄: 19–10 @ 298 K), and [Co₂(tzpa)(OH)(H₂O)₂]_n (CO₂/CH₄: 54–35 @ 298 K and 34–20 @ 313 K).^{49–67} The literature survey of CO₂/N₂ and CO₂/CH₄ selectivity based on different temperatures, pressures, and compositions is summarized in Table S4. Along with selectivity, the evaluation of the adsorbed amount of the desired gas in a mixed gas phase is very much emergent to evaluate the capability of 1' in the pressure-swing adsorption unit. The CO₂ loading receptivity values for 1' in the mixed gas phase (CO₂/N₂ = 15:85) at equilibrium are 0.57, 0.675, and 0.767 mmol g⁻¹ at 313, 305, and 298 K, respectively. These values are higher than those for other MOF-based systems such as MOF-177 (0.16 mmol g⁻¹ at 295 K; 100 kPa for CO₂/N₂), IITKGP-6a (0.33 mmol g⁻¹ at 295 K; 100 kPa for CO₂/N₂), and [Zn₄(FMA)₃] (0.26 mmol g⁻¹ at 295 K; 100 kPa for CO₂/N₂) (Figure 5).^{54,64} On the other hand, for a 50:50 CO₂/CH₄ mixed gas phase at equilibrium, the values for 1' are 0.92, 1.109, and 1.26 mmol g⁻¹ at 313, 305, and 298 K, respectively (Figure 5), which are higher than other MOF-based systems such as [Zn₄(FMA)₃] (1.07 mmol g⁻¹ at 296 K; 2 bar for CO₂/CH₄), zeolite MFI (0.89 mmol g⁻¹ at 296 K; 2 bar for CO₂/CH₄), and IITKGP-6a (0.77 mmol g⁻¹ at 295 K).^{54,64}

Recyclability Test of 1' for CO₂ Capture. For a practical application, it is desirable to check the efficiency of a material in gas uptake and separation for repetitive times. In order to investigate this, CO₂ sorption measurements were carried out at 298 K and 1 bar pressure using 1' as an adsorbent for five consecutive cycles. Prior to each cycle, 1' was degassed at 120 °C for 24 h under high vacuum. Based on the data shown in Figure S22, it is evident that 1' has the potential to regain its original uptake capacity for CO₂ up to five cycles (33.6 to 32.4

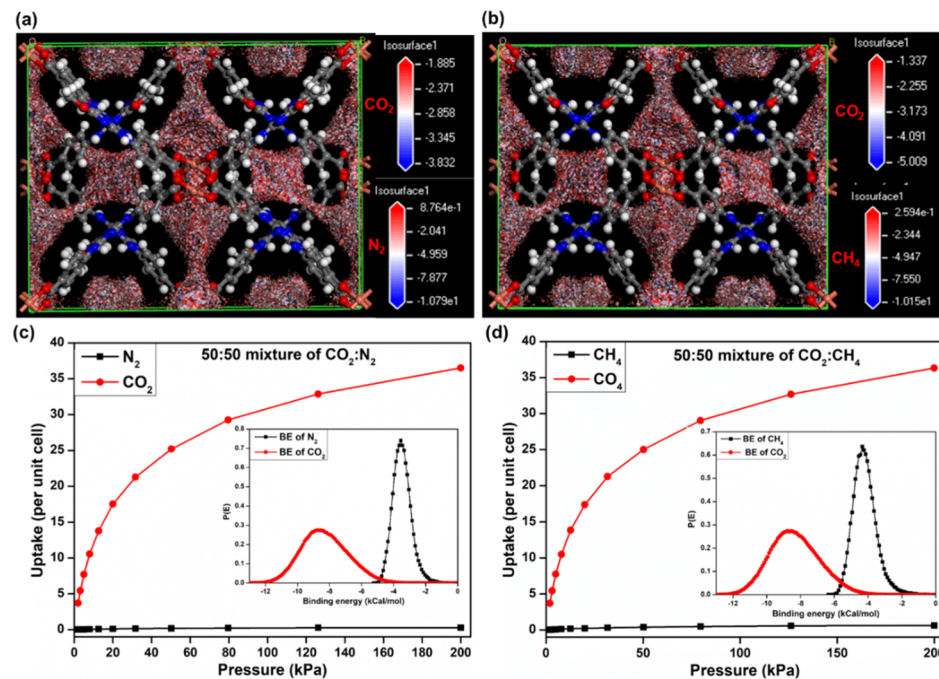


Figure 7. CO₂ separation over N₂ and CH₄ by CBMC simulation: density distribution map of (a) CO₂/N₂ (50:50) and (b) CO₂/CH₄ (50:50) mixture at 313 K. (c,d) Uptake selectivity and BEs at 313 K for the 50:50 mixtures.

cm³ g⁻¹). This demonstrates that **1'** is an efficient material for CO₂ sorption studies.

Computational Analysis. To gain a deeper insight into the very high selectivity for CO₂ over other gases, quantum computational studies were carried out by employing CBMC molecular simulation in BIOVIA, Materials Studio 2018R2. At first, CO₂, N₂, and CH₄ sorption analyses have been computed within **1'** framework containing (1 × 1 × 1) unit cells at 313 K up to fixed pressure 1 bar (Figure 6). From this study, the number of CO₂, CH₄, and N₂ molecules present per unit cell is found to be 33, 4, and 2, respectively. This high CO₂ capture at high temperature follows the experimental results (Figure 6a–c). Furthermore, it was clearly evident that there were strong dipole–quadrupole and quadrupole–quadrupole interactions with high binding energy (BE = −36 kJ/mol at 313 K) for CO₂ (Figure 6d).^{33,63–65} The intermolecular distances between CO₂ and the copper center in **1'** are 3.13 and 2.66 Å at 313 and 195 K, respectively. The CO₂ molecule interacts further with the methoxy group of another undulated layer (Figure S23a,e). The electronegative O atom and electropositive C atom of CO₂ interact with N–H (O···H–N = 2.02 Å) and triazine N (C–O···N = 3.6 Å) of ligand in the channel of two undulated layers (Figure S23e). These results are highly comparable with other functional MOFs such as Co₂(tzpa) (2.4–3.7 Å),⁵ SMOF-SIFSix-1a (3.4–3.8 Å),⁶⁷ UTSA-16 (2.9–3 Å),⁴⁸ and so forth. Also, we have performed the CO₂ uptake at different temperatures and the position of CO₂ has been shown in Figure S23. Mainly, the OMSs of Cu(II) paddle-wheel units and polar amine and methoxy groups exhibit strong interactions with CO₂ molecules.

Similarly, the uptake and position of CH₄ has been shown at different temperatures (Figure S24). Also, it is noteworthy to see that the BE for CO₂ is exceedingly high compared to that of N₂ (BE = −11 kJ/mol) and CH₄ (BE = −17 kJ/mol) and thereby resulting in higher CO₂ uptake (Figure 6d). From a practical application viewpoint with respect to the separation

of mixed gases, CBMC simulation was performed for CO₂/N₂ (50:50) and CO₂/CH₄ (50:50) at 313 and 298 K up to 1 bar (Figures 7 and S25). Both loading and BE for CO₂ are found to be very high with excellent selectivity over that of N₂ and CH₄. This study is also in well-correlation with the aforesaid experimental results. With further in-depth exploration into the density distribution map, it is notable that the contribution for CO₂ is higher than N₂ and CH₄ at 313 and 298 K as evident from the isosurface values (Figures 7a,b and S25a,b). Additionally, the simulated uptake isotherms for 50:50 CO₂/N₂ and 50:50 CO₂/CH₄ mixtures depict high affinity toward CO₂ compared to N₂ and CH₄ at 313 and 298 K up to pressure 200 kPa (Figures 7a,b and S25). Consequently, the simulated BE of CO₂ is much higher in comparison to N₂ and CH₄ in a mixture of gases, which matches with the experimental results (Figure 7c,d).

CO₂ Chemical Fixation under Ambient Conditions. The high CO₂ uptake encouraged us further to utilize **1'** as a heterogeneous catalyst for CO₂ fixation via the cycloaddition reaction with epoxides. Initial screening experiments were carried out to establish the requirements of the catalyst and tetrabutylammonium bromide (TBAB or "Bu₄NBr") as a cocatalyst for the cycloaddition of CO₂ with epichlorohydrin using CO₂ balloon pressure for 24 h under ambient conditions. Using both **1'** (0.1 mol %) and TBAB (0.5 mol %) without a solvent, the reaction affords >98% conversion. On the other hand, using (a) only TBAB or "Bu₄NBr" but no **1'** and (b) only **1'** without TBAB, the reaction affords 28 and 0% conversion, respectively (Table S5). These results depict that the cycloaddition of CO₂ with epichlorohydrin can be obtained in high yield by the synergistic utilization of **1'** and the cocatalyst TBAB under ambient conditions.^{15,44–46,68–70} Based on this, other substrates with smaller and larger substituents were also investigated. With 0.1 mol % of **1'** and 0.5 mol % TBAB, an efficient catalytic activity was observed with yields 60–98% (Figures S26–S33). The effect of halobenzene-based

epoxides was also considered for the cycloaddition reaction of CO₂. It is clearly evident that for the 2-(4-bromophenyl)-oxirane substrate, an excellent conversion (Table 1, entry 4)

Table 1. CO₂ Cycloaddition: Epoxide to Cyclic Carbonates

Entry	R	Product	Conversion ^a (%)	TON
1			68	681
2			76	763
3			78	778
4			94	941
5			66	662
6			>99	995
7			>99	1000
8			60	602

^aCalculated using ¹H NMR spectroscopy.

was acquired compared to the 3- or 4-chloro derivatives (Table 1, entries 2 and 3, respectively). However, when larger substrates with a butyl chain were used, comparatively low % conversion (60%) was obtained under the same conditions because of the steric hindrance effect (Table 1, entry 8). Also, the corresponding turn over number for different substrates in this study is comparable with other reported MOFs.^{68–70} Thus, these results demonstrate that 1' serves as an effective heterogeneous catalyst with size-selective conversion.

The recyclability test for 1' was also examined by utilizing epichlorohydrin as a representative substrate to carry out the catalysis. After the reaction, the spent catalyst was regenerated by centrifugation, filtration, washing, and vacuum drying. Following the same protocol, 1' was regenerated for four consecutive cycles and its catalytic activity was determined. It is noteworthy to observe that 1' retains its native catalytic activity without any significant change in it throughout the process with yields >95% (Figures S34 and S35).

Plausible Mechanisms for CO₂ Cycloaddition with Epoxides. Two plausible mechanisms for CO₂ cycloaddition to epoxides catalyzed by 1' has been proposed based on the features present in the framework as well as earlier literature reports^{44,45,68–71} (Figure 8). Two types of active sites in 1' coexist to efficiently activate the epoxide substrates: (i) accessible OMSs (Lewis acidic Cu(II)) in the paddle-wheel units, and (ii) Brønsted acid sites from secondary amine moieties. To investigate further about the interaction sites of epoxide with 1', computational studies were performed using the CBMC simulation between 1' and propylene oxide (PO). The CBMC simulation depicts a strong interaction with Lewis acidic paddle wheel copper and O of PO (Cu···O(PO) = 2.14 Å). Also, a H-bonding interaction was observed between C–O of PO and N–H of 1' (O···N = 2.25 Å) (Figure S36). Accordingly, the Lewis acidic Cu(II) centers and basic –NH moieties of 1' simultaneously get involved in the coordination with the oxygen atom (O) of PO to initiate the reaction.

After that, the Br⁻ ion of the cocatalyst ^tBu₄N⁺Br⁻ undergoes a nucleophilic attack on the less-crowded carbon atom of the epoxide allowing its ring opening. The reaction between the O atom of the ring-opened epoxide and CO₂ generates metal-carbonate and hydrogen-bonded carbonate intermediates. Ultimately, a cyclic carbonate is formed via an intramolecular ring closing reaction followed by the regeneration of the catalyst. These two mechanistic pathways for 1' reveal a synergistic effect due to the presence of both active Lewis acid and Brønsted acid sites that play an important role in stimulating the reaction.

CONCLUSIONS

In summary, a new parallel polycatenated undulated 3D Cu-MOF (1) with a paddle-wheel core was successfully synthesized under solvothermal condition using a new multifunctional triazine-based dicarboxylic acid. It shows extraordinary thermal and chemical stability in water as well as in the presence of other reacting solvents. The OMSs and heteroatoms (amine, methoxy, and triazine) anchored in the pore walls of 1 make this material a potential candidate for gas storage and separation application. The incorporation of active OMSs and polar Brønsted acidic functional groups paved the way for significant CO₂ sorption. 1' showcases high CO₂ capture under ambient conditions, reflected in a high Q_{st} value compared to those for N₂ and CH₄. The highly selective CO₂ capture and separation at high temperature over N₂ and CH₄ by 1' amplified its potential toward flue gas and landfill gas separation. Moreover, the CBMC molecular simulation displays the interaction sites, BE, high capture, and selectivity of CO₂ over other gases at different temperatures. Significantly, 1' is also shown as an excellent bifunctional heterogeneous

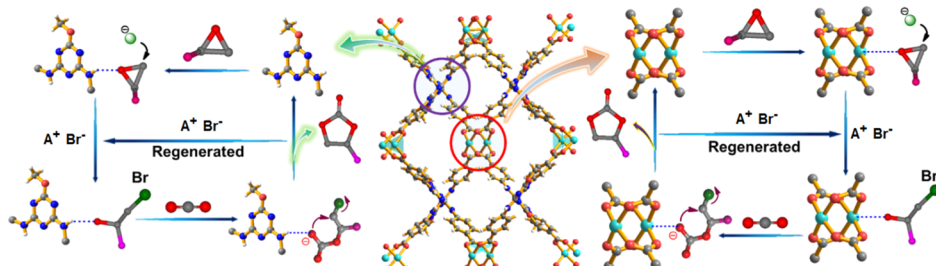


Figure 8. Two plausible mechanisms for the CO₂ cycloaddition reaction catalyzed by 1' (A⁺ = tetrabutyl ammonium ion).

catalyst for the chemical fixation of CO₂. Under ambient conditions, 1' shows high to moderate yield based on size selectivity. Its mechanistic pathways have been explained based on the CBMC simulations as well. Thus, the highly stable Cu-MOF represents an auspicious porous material for high temperature CO₂ capture, separation, and chemical fixation to value-added cyclic carbonates and thereby contributing to extenuate the issue of global climate.

EXPERIMENTAL SECTION

Materials and methods have been described in the [Supporting Information](#).

ASSOCIATED CONTENT

Supporting Information

The Supporting Information is available free of charge at <https://pubs.acs.org/doi/10.1021/acsami.0c09024>.

Synthesis and structural characterization, DLSF fitting, comparison tables, CBMC simulation, and NMR spectra for catalysis ([PDF](#))

Crystallographic information file (CCDC no. 1999264 (1)) ([CIF](#))

AUTHOR INFORMATION

Corresponding Author

Sanjay K. Mandal — Department of Chemical Sciences, Indian Institute of Science Education and Research Mohali, Mohali, Punjab 140306, India;  orcid.org/0000-0002-5045-6343;
Email: sanjaymandal@iisermohali.ac.in

Author

Prasenjit Das — Department of Chemical Sciences, Indian Institute of Science Education and Research Mohali, Mohali, Punjab 140306, India

Complete contact information is available at:
<https://pubs.acs.org/10.1021/acsami.0c09024>

Notes

The authors declare no competing financial interest.

ACKNOWLEDGMENTS

This work was funded by the IISER Mohali. P.D. is highly obliged to the MHRD of India for providing a fellowship. Authors acknowledge the central as well as departmental facilities at the IISER Mohali.

REFERENCES

- (1) CO₂ Emissions from Fuel Combustion Highlights (2015 Edition); OECD/IEA, 2015.
- (2) Singh, D.; Croiset, E.; Douglas, P. L.; Douglas, M. A. Techno-economic study of CO₂ capture from an existing coal-fired power plant: MEA scrubbing vs O₂/CO₂ recycle combustion. *Energy Convers. Manage.* **2003**, *44*, 3073.
- (3) Chu, S. Carbon Capture and Sequestration. *Science* **2009**, *325*, 1599.
- (4) Kondratenko, E. V.; Mul, G.; Baltrusaitis, J.; Larrazábal, G. O.; Pérez-Ramírez, J. Status and perspectives of CO₂ conversion into fuels and chemicals by catalytic, photocatalytic and electrocatalytic processes. *Energy Environ. Sci.* **2013**, *6*, 3112–3135.
- (5) Wang, H.-H.; Hou, L.; Li, Y.-Z.; Jiang, C.-Y.; Wang, Y.-Y.; Zhu, Z. Porous MOF with Highly Efficient Selectivity and Chemical Conversion for CO₂. *ACS Appl. Mater. Interfaces* **2017**, *9*, 17969–17976.
- (6) Habib, M. A.; Nemitalah, M.; Ben-Mansour, R. Recent Development in Oxy-Combustion Technology and Its Applications to Gas Turbine Combustors and ITM Reactors. *Energy Fuels* **2013**, *27*, 2–19.
- (7) Lin, L.-C.; Berger, A. H.; Martin, R. L.; Kim, J.; Swisher, J. A.; Jariwala, K.; Rycroft, C. H.; Bhowm, A. S.; Deem, M. W.; Haranczyk, M.; Smit, B. In Silico Screening of Carbon-Capture Materials. *Nat. Mater.* **2012**, *11*, 633–641.
- (8) Haszeldine, R. S. Carbon Capture and Storage: How Green Can Black Be? *Science* **2009**, *325*, 1647–1652.
- (9) Patel, H. A.; Je, S. H.; Park, J.; Chen, D. P.; Jung, Y.; Yavuz, C. T.; Coskun, A. Unprecedented High-Temperature CO₂ Selectivity in N₂-phobic Nanoporous Covalent Organic Polymers. *Nat. Commun.* **2013**, *4*, 1357.
- (10) Sakakura, T.; Kohno, K. The Synthesis of Organic Carbonates from Carbon Dioxide. *Chem. Commun.* **2009**, 1312–1330.
- (11) North, M.; Pasquale, R.; Young, C. Synthesis of Cyclic Carbonates from Epoxides and CO₂. *Green Chem.* **2010**, *12*, 1514–1539.
- (12) Dai, W.-L.; Luo, S.-L.; Yin, S.-F.; Au, C.-T. The Direct Transformation of Carbon Dioxide to Organic Carbonates Over Heterogeneous Catalysts. *Appl. Catal., A* **2009**, *366*, 2–12.
- (13) Yoshida, M.; Ihara, M. Novel Methodologies for the Synthesis of Cyclic Carbonates. *Chem.—Eur. J.* **2004**, *10*, 2886–2893.
- (14) Zhang, S. S. A review on electrolyte additives for lithium-ion batteries. *J. Power Sources* **2006**, *162*, 1379–1394.
- (15) Gao, W.-Y.; Chen, Y.; Niu, Y.; Williams, K.; Cash, L.; Perez, P. J.; Wojtas, L.; Cai, J.; Chen, Y.-S.; Ma, S. Crystal Engineering of an nbo Topology Metal-Organic Framework for Chemical Fixation of CO₂ under Ambient Conditions. *Angew. Chem., Int. Ed.* **2014**, *53*, 2615–2619.
- (16) Li, P.-Z.; Wang, X.-J.; Liu, J.; Lim, J. S.; Zou, R.; Zhao, Y. A Triazole-Containing Metal-Organic Framework as a Highly Effective and Substrate Size-Dependent Catalyst for CO₂ Conversion. *J. Am. Chem. Soc.* **2016**, *138*, 2142–2145.
- (17) He, H.; Sun, Q.; Gao, W.; Perman, J. A.; Sun, F.; Zhu, G.; Aguila, B.; Forrest, K.; Space, B.; Ma, S. A Stable Metal–Organic Framework Featuring a Local Buffer Environment for Carbon Dioxide Fixation. *Angew. Chem., Int. Ed.* **2018**, *57*, 4657–4662.
- (18) Das, S. K.; Bhanja, P.; Kundu, S. K.; Mondal, S.; Bhaumik, A. Role of Surface Phenolic-OH Groups in N-Rich Porous Organic Polymers for Enhancing the CO₂ Uptake and CO₂/N₂ Selectivity: Experimental and Computational Studies. *ACS Appl. Mater. Interfaces* **2018**, *10*, 23813–23824.
- (19) Pardakhti, M.; Jafari, T.; Tobin, Z.; Dutta, B.; Moharreri, E.; Shemshaki, N. S.; Suib, S.; Srivastava, R. Trends in Solid Adsorbent Materials Development for CO₂ Capture. *ACS Appl. Mater. Interfaces* **2019**, *11*, 34533–34559.
- (20) Lu, W.; Wei, Z.; Gu, Z.-Y.; Liu, T.-F.; Park, J.; Park, J.; Tian, J.; Zhang, M.; Zhang, Q.; Gentle, T., III; Bosch, M.; Zhou, H.-C. Tuning the structure and function of metal–organic frameworks via linker design. *Chem. Soc. Rev.* **2014**, *43*, 5561–5593.
- (21) Cui, X.; Chen, K.; Xing, H.; Yang, Q.; Krishna, R.; Bao, Z.; Wu, H.; Zhou, W.; Dong, X.; Han, Y.; Li, B.; Ren, Q.; Zaworotko, M. J.; Chen, B. Pore Chemistry and Size Control in Hybrid Porous Materials for Acetylene Capture From Ethylene. *Science* **2016**, *353*, 141.
- (22) Assen, A. H.; Belmabkhout, Y.; Adil, K.; Bhatt, P. M.; Xue, D.-X.; Jiang, H.; Eddaoudi, M. Ultra-Tuning of the Rare-Earth fcu-MOF Aperture Size for Selective Molecular Exclusion of Branched Paraffins. *Angew. Chem., Int. Ed.* **2015**, *54*, 14353–14358.
- (23) Wang, Q.; Bai, J.; Lu, Z.; Pan, Y.; You, X. Finely Tuning MOFs Towards High-Performance Post-Combustion CO₂ Capture Materials. *Chem. Commun.* **2016**, *52*, 443–452.
- (24) Li, L.; Tang, S.; Wang, C.; Lv, X.; Jiang, M.; Wu, H.; Zhao, X. High Gas Storage Capacities and Stepwise Adsorption in a UiO Type Metal-Organic Framework Incorporating Lewis Basic Bipyridyl Sites. *Chem. Commun.* **2014**, *50*, 2304–2307.

- (25) Bao, S.-J.; Krishna, R.; He, Y.-B.; Qin, J.-S.; Su, Z.-M.; Li, S.-L.; Xie, W.; Du, D.-Y.; He, W.-W.; Zhang, S.-R.; Lan, Y.-Q. A Stable Metal–Organic Framework with Suitable Pore Sizes and Rich Uncoordinated Nitrogen Atoms on the Internal Surface of Micropores for Highly Efficient CO₂ Capture. *J. Mater. Chem. A* **2015**, *3*, 7361–7367.
- (26) Farha, O. K.; Eryazici, I.; Jeong, N. C.; Hauser, B. G.; Wilmer, C. E.; Sarjeant, A. A.; Snurr, R. Q.; Nguyen, S. T.; Yazaydin, A. Ö.; Hupp, J. T. Metal–Organic Framework Materials with Ultrahigh Surface Areas: Is the Sky the Limit? *J. Am. Chem. Soc.* **2012**, *134*, 15016–15021.
- (27) Wang, T. C.; Bury, W.; Gómez-Gualdrón, D. A.; Vermeulen, N. A.; Mondloch, J. E.; Deria, P.; Zhang, K.; Moghadam, P. Z.; Sarjeant, A. A.; Snurr, R. Q.; Stoddart, J. F.; Hupp, J. T.; Farha, O. K. Ultrahigh Surface Area Zirconium MOFs and Insights into the Applicability of the BET Theory. *J. Am. Chem. Soc.* **2015**, *137*, 3585–3591.
- (28) Tan, Y.-X.; Wang, F.; Zhang, J. Design and Synthesis of Multifunctional Metal–Organic Zeolites. *Chem. Soc. Rev.* **2018**, *47*, 2130–2144.
- (29) Wang, S.; Belmabkhout, Y.; Cairns, A. J.; Li, G.; Huo, Q.; Liu, Y.; Eddaoudi, M. Tuning Gas Adsorption Properties of Zeolite-like Supramolecular Assemblies with gis Topology Via Functionalization of Isoreticular Metal–Organic Squares. *ACS Appl. Mater. Interfaces* **2017**, *9*, 33521–33527.
- (30) Xiong, Y.; Fan, Y.-Z.; Yang, R.; Chen, S.; Pan, M.; Jiang, J.-J.; Su, C.-Y. Amide and N-oxide Functionalization of T-shaped Ligands for Isoreticular MOFs with Giant Enhancements in CO₂ Separation. *Chem. Commun.* **2014**, *50*, 14631–14634.
- (31) Ajaz, A.; Akita, T.; Yang, H.; Xu, Q. From Ionic-Liquid@Metal–Organic Framework Composites to Heteroatom Decorated Large-Surface Area Carbons: Superior CO₂ and H₂ Uptake. *Chem. Commun.* **2014**, *50*, 6498–6501.
- (32) Kirchon, A.; Feng, L.; Drake, H. F.; Joseph, E. A.; Zhou, H.-C. From fundamentals to applications: a toolbox for robust and multifunctional MOF materials. *Chem. Soc. Rev.* **2018**, *47*, 8611–8638.
- (33) Adil, K.; Belmabkhout, Y.; Pillai, R. S.; Cadiou, A.; Bhatt, P. M.; Assen, A. H.; Maurin, G.; Eddaoudi, M. Gas/Vapour Separation Using Ultra-Microporous Metal–Organic Frameworks: Insights into the Structure/Separation Relationship. *Chem. Soc. Rev.* **2017**, *46*, 3402–3430.
- (34) Sumida, K.; Rogow, D. L.; Mason, J. A.; McDonald, T. M.; Bloch, E. D.; Herm, Z. R.; Bae, T.-H.; Long, J. R. Carbon Dioxide Capture in Metal–Organic Frameworks. *Chem. Rev.* **2012**, *112*, 724–781.
- (35) Liang, L.; Liu, C.; Jiang, F.; Chen, Q.; Zhang, L.; Xue, H.; Jiang, H.; Qian, J.; Yuan, D.; Hong, M. Carbon Dioxide Capture and Conversion by an Acid–Base Resistant Metal–Organic Framework. *Nat. Commun.* **2017**, *8*, 1233.
- (36) Chen, C.-X.; Zheng, S.-P.; Wei, Z.-W.; Cao, C.-C.; Wang, H.-P.; Wang, D.; Jiang, J.-J.; Fenske, D.; Su, C.-Y. A Robust Metal–Organic Framework Combining Open Metal Sites and Polar Groups for Methane Purification and CO₂/Fluorocarbon Capture. *Chem.—Eur. J.* **2017**, *23*, 4060–4064.
- (37) Li, X.-Y.; Li, Y.-Z.; Yang, Y.; Hou, L.; Wang, Y.-Y.; Zhu, Z. Efficient Light Hydrocarbon Separation and CO₂ Capture and Conversion in a Stable MOF with Oxalamide-Decorated Polar Tubes. *Chem. Commun.* **2017**, *53*, 12970–12973.
- (38) Cui, P.; Ma, Y.-G.; Li, H.-H.; Zhao, B.; Li, J.-R.; Cheng, P.; Balbuena, P. B.; Zhou, H.-C. Multipoint Interactions Enhanced CO₂ Uptake: A Zeolite-Like Zinc-Tetrazole Framework with 24-Nuclear Zinc Cages. *J. Am. Chem. Soc.* **2012**, *134*, 18892–18895.
- (39) Ma, H.-F.; Liu, Q.-Y.; Wang, Y.-L.; Yin, S.-G. A Water-Stable Anionic Metal–Organic Framework Constructed from Columnar Zinc-Adeninate Units for Highly Selective Light Hydrocarbon Separation and Efficient Separation of Organic Dyes. *Inorg. Chem.* **2017**, *56*, 2919–2925.
- (40) Duan, J.; Higuchi, M.; Zheng, J.; Noro, S.-i.; Chang, I.-Y.; Hyeon-Deuk, K.; Mathew, S.; Kusaka, S.; Sivaniah, E.; Matsuda, R.; Sakaki, S.; Kitagawa, S. Density Gradation of Open Metal Sites in the Mesospace of Porous Coordination Polymers. *J. Am. Chem. Soc.* **2017**, *139*, 11576–11583.
- (41) Marti, R. M.; Howe, J. D.; Morelock, C. R.; Conradi, M. S.; Walton, K. S.; Sholl, D. S.; Hayes, S. E. CO₂ Dynamics in Pure and Mixed-Metal MOFs with Open Metal Sites. *J. Phys. Chem. C* **2017**, *121*, 25778–25787.
- (42) Jiang, H.-L.; Makal, T. A.; Zhou, H.-C. Interpenetration Control in Metal–Organic Frameworks for Functional Applications. *Coord. Chem. Rev.* **2013**, *257*, 2232–2249.
- (43) Gao, W.-Y.; Chen, Y.; Niu, Y.; Williams, K.; Cash, L.; Perez, P. J.; Wojtas, L.; Cai, J.; Chen, Y.-S.; Ma, S. Crystal Engineering of an Nbo Topology Metal–Organic Framework for Chemical Fixation of CO₂ Under Ambient Conditions. *Angew. Chem., Int. Ed.* **2014**, *53*, 2615–2619.
- (44) Beyzavi, M. H.; Klet, R. C.; Tussupbayev, S.; Borycz, J.; Vermeulen, N. A.; Cramer, C. J.; Stoddart, J. F.; Hupp, J. T.; Farha, O. K. A Hafnium-Based Metal–Organic Framework as an Efficient and Multifunctional Catalyst for Facile CO₂ Fixation and Regioselective and Enantioselective Epoxide Activation. *J. Am. Chem. Soc.* **2014**, *136*, 15861–15864.
- (45) Li, P.-Z.; Wang, X.-J.; Liu, J.; Lim, J. S.; Zou, R.; Zhao, Y. A Triazole-Containing Metal–Organic Framework as a Highly Effective and Substrate Size-Dependent Catalyst for CO₂ Conversion. *J. Am. Chem. Soc.* **2016**, *138*, 2142–2145.
- (46) Ding, M.; Flraig, R. W.; Jiang, H.-L.; Yaghi, O. M. Carbon capture and conversion using metal–organic frameworks and MOF-based materials. *Chem. Soc. Rev.* **2019**, *48*, 2783–2828.
- (47) Nakamoto, K. *Infrared and Raman Spectra of Inorganic and Coordination Compounds*, 5th ed.; John Wiley and Sons: New York, 1997.
- (48) Xiang, S.; He, Y.; Zhang, Z.; Wu, H.; Zhou, W.; Krishna, R.; Chen, B. Microporous metal–organic framework with potential for carbon dioxide capture at ambient conditions. *Nat. Commun.* **2012**, *3*, 954.
- (49) Dunn, T. M. *The Visible and Ultraviolet Spectra of Complex Compounds in Modern Coordination Chemistry*; Interscience: New York, 1960.
- (50) Yang, S.; Lin, X.; Blake, A. J.; Walker, G. S.; Hubberstey, P.; Champness, N. R.; Schröder, M. Cation-Induced Kinetic Trapping and Enhanced Hydrogen Adsorption in a Modulated Anionic Metal–Organic Framework. *Nat. Chem.* **2009**, *1*, 487–493.
- (51) Li, B.; Zhang, Z.; Li, Y.; Yao, K.; Zhu, Y.; Deng, Z.; Yang, F.; Zhou, X.; Li, G.; Wu, H.; Nijem, N.; Chabal, Y. J.; Lai, Z.; Han, Y.; Shi, Z.; Feng, S.; Li, J. Enhanced Binding Affinity, Remarkable Selectivity, and High Capacity of CO₂ by Dual Functionalization of a rht-Type Metal–Organic Framework. *Angew. Chem., Int. Ed.* **2012**, *51*, 1412–1415.
- (52) Feng, G.; Peng, Y.; Liu, W.; Chang, F.; Dai, Y.; Huang, W. Polar Ketone-Functionalized Metal–Organic Framework Showing a High CO₂ Adsorption Performance. *Inorg. Chem.* **2017**, *56*, 2363–2366.
- (53) Zheng, B.; Bai, J.; Duan, J.; Wojtas, L.; Zaworotko, M. J. Enhanced CO₂ Binding Affinity of a High-Uptake rht-Type Metal–Organic Framework Decorated with Acylamide Groups. *J. Am. Chem. Soc.* **2011**, *133*, 748–751.
- (54) Pal, A.; Chand, S.; Das, M. C. A Water Stable Two-Fold Interpenetrating Microporous MOF for Selective CO₂ Adsorption and Separation. *Inorg. Chem.* **2017**, *56*, 13991–13997.
- (55) Yang, S.; Lin, X.; Lewis, W.; Suyetin, M.; Bichoutskaia, E.; Parker, J. E.; Tang, C. C.; Allan, D. R.; Rizkallah, P. J.; Hubberstey, P.; Champness, N. R.; Mark Thomas, K.; Blake, A. J.; Schröder, M. Partially Interpenetrated Metal–Organic Framework for Selective Hysteretic Sorption of Carbon Dioxide. *Nat. Mater.* **2012**, *11*, 710–716.
- (56) Wang, H.-H.; Hou, L.; Li, Y.-Z.; Jiang, C.-Y.; Wang, Y.-Y.; Zhu, Z. Porous MOF with Highly Efficient Selectivity and Chemical Conversion for CO₂. *ACS Appl. Mater. Interfaces* **2017**, *9*, 17969–17976.

- (57) Myers, A. L.; Prausnitz, J. M. Thermodynamics of mixed-gas adsorption. *AIChE J.* **1965**, *11*, 121–127.
- (58) Li, Z.; Feng, X.; Zou, Y.; Zhang, Y.; Xia, H.; Liu, X.; Mu, Y. A 2D Azine-Linked Covalent Organic Framework for Gas Storage Applications. *Chem. Commun.* **2014**, *50*, 13825–13828.
- (59) Gao, Q.; Li, X.; Ning, G.-H.; Xu, H.-S.; Liu, C.; Tian, B.; Tang, W.; Loh, K. P. Covalent Organic Framework with Frustrated Bonding Network for Enhanced Carbon Dioxide Storage. *Chem. Mater.* **2018**, *30*, 1762–1768.
- (60) Gao, W.-Y.; Yan, W.; Cai, R.; Williams, K.; Salas, A.; Wojtas, L.; Shi, X.; Ma, S. A Pillared Metal–Organic Framework Incorporated with 1,2,3-Triazole Moieties Exhibiting Remarkable Enhancement of CO₂ Uptake. *Chem. Commun.* **2012**, *48*, 8898–8900.
- (61) Kuhn, P.; Antonietti, M.; Thomas, A. Porous, Covalent Triazine-Based Frameworks Prepared by Ionothermal Synthesis. *Angew. Chem., Int. Ed.* **2008**, *47*, 3450–3453.
- (62) Tao, L.; Niu, F.; Wang, C.; Liu, J.; Wang, T.; Wang, Q. Benzimidazole Functionalized Covalent Triazine Frameworks for CO₂ Capture. *J. Mater. Chem. A* **2016**, *4*, 11812–11820.
- (63) Ben, T.; Pei, C.; Zhang, D.; Xu, J.; Deng, F.; Jing, X.; Qiu, S. Gas Storage in Porous Aromatic Frameworks (PAFs). *Energy Environ. Sci.* **2011**, *4*, 3991–3999.
- (64) Xiang, S.; He, Y.; Zhang, Z.; Wu, H.; Zhou, W.; Krishna, R.; Chen, B. Microporous Metal–Organic Framework with Potential for Carbon Dioxide Capture at Ambient Conditions. *Nat. Commun.* **2012**, *3*, 954–963.
- (65) Das, P.; Mandal, S. K. In-Depth Experimental and Computational Investigations for Remarkable Gas/Vapor Sorption, Selectivity, and Affinity by a Porous Nitrogen-Rich Covalent Organic Framework. *Chem. Mater.* **2019**, *31*, 1584–1596.
- (66) Chakraborty, G.; Das, P.; Mandal, S. K. Polar Sulfone-Functionalized Oxygen-Rich Metal–Organic Frameworks for Highly Selective CO₂ Capture and Sensitive Detection of Acetylacetone at ppb Level. *ACS Appl. Mater. Interfaces* **2020**, *12*, 11724–11736.
- (67) Dai, J.; Xie, D.; Liu, Y.; Zhang, Z.; Yang, Y.; Yang, Q.; Ren, Q.; Bao, Z. Supramolecular Metal–Organic Framework for CO₂/CH₄ and CO₂/N₂ Separation. *Ind. Eng. Chem. Res.* **2020**, *59*, 7866–7874.
- (68) Rowsell, J. L. C.; Yaghi, O. M. Effects of Functionalization, Catenation, and Variation of the Metal Oxide and Organic Linking Units on the Low-Pressure Hydrogen Adsorption Properties of Metal–Organic Frameworks. *J. Am. Chem. Soc.* **2006**, *128*, 1304–1315.
- (69) Li, P.-Z.; Wang, X.-J.; Liu, J.; Lim, J. S.; Zou, R.; Zhao, Y. A Triazole-Containing Metal–Organic Framework as a Highly Effective and Substrate Size-Dependent Catalyst for CO₂ Conversion. *J. Am. Chem. Soc.* **2016**, *138*, 2142–2145.
- (70) Xie, Y.; Wang, T.-T.; Liu, X.-H.; Zou, K.; Deng, W.-Q. Capture and conversion of CO₂ at ambient conditions by a conjugated microporous polymer. *Nat. Commun.* **2013**, *4*, 1960.
- (71) Wang, J.; Zhang, Y. Boronic Acids as Hydrogen Bond Donor Catalysts for Efficient Conversion of CO₂ into Organic Carbonate in Water. *ACS Catal.* **2016**, *6*, 4871–4876.